High-Field 285 GHz Electron Paramagnetic Resonance Study of Indigenous Radicals of Humic Acids

Konstantinos C. Christoforidis,[†,‡] Sun Un,[*,‡] and Yiannis Deligiannakis[*,†]

Laboratory of Physical Chemistry, Department of Environmental and Natural Resources Management, University of Ioannina, Seferi 2, 30100 Agrinio, Greece, and Service de Bioenergetique, CEA Saclay, 91191 Gif-Sur-Yvette, France

Received: March 5, 2007; In Final Form: August 10, 2007

Humic substances, the largest source of carbon on Earth, contain indigenous stable free radicals that are involved in important biogeochemical environmental processes occurring in soil and water systems. Here, we present the first high-magnetic-field 285GHz electron paramagnetic resonance spectra for humic acids from various geographical origins. All humic acids irrespective of their origin contain two limiting types of indigenous stable radicals, types I and II, with distinct electronic structure. Type I, which prevails at acidic pH 5, is characterized by a **g** tensor with principal values $g^{I}_{x} = 2.0032$, $g^{I}_{y} = 2.0032$, and $g^{I}_{z} = 2.0023$. Type II, which prevails at alkaline pH 12, is characterized by $g^{II}_{x} = 2.0057$, $g^{II}_{y} = 2.0055$, and $g^{II}_{z} = 2.0023$. The two limiting types are correlated in a unified reversible manner with pH, irrespective of the geographic origin of the HA. Both types of radical centers are consistent with π-type radicals. They persist not only in liquid solutions but also in humic acid powders.

1. Introduction

Humic acids (HAs) being the most abundant class of organic substances in soils are one of the largest sources of abiotic carbon on Earth.[1] HAs are responsible for some of the fundamental physicochemical environmental properties of soils[1−3] such as stabilization, mobilization, redox transformation of organic material, and complexation of metal ions.[3] All HAs regardless of their geographic and climatic origins contain stable organic radical moieties[4,5] that are indigenous to the HA structure[1,4−6] and involved in important biochemical[1,6,7] and chemical[1,6,8−17] environmental processes, including the transformation of HAs themselves,[9] the degradation of organics,[1,9,14] or the humification process in natural soil[1,2,15] and compost.[16]

For example, HAs can act as electron acceptors from soil microorganisms for the anaerobic oxidation of organic compounds and hydrogen.[7] Formation of elemental mercury can be efficiently mediated by humic acid through radical reactions.[8] Due to their phenolic groups, HAs can be photoexcited,[9] generating radicals which mediate the transformation of humic acid itself[10] or the degradation of organic compounds.[1,10,14] Most importantly, the indigenous radicals of HA are determining factors of the humification process in natural soil[1,2,15] and compost.[16] However, the details of this mechanism are not fully understood. There is strong evidence that polyphenols[17−19] present in terrestrial and aquatic environments can be important precursors for the formation of humic substances[1] via radical polymerization which takes place in soils and sediments.[17−19] Despite the progress in this front, fundamental questions concerning the molecular identity, the electronic properties, and the diversity of the indigenous radicals in HAs have always been the subject of contention. These points have been extensively discussed in the literature.[1,2,4,7,11−13]

Electron paramagnetic resonance (EPR) has been the method of choice for the detection and quantification of radicals in HAs.[2,6] The application of EPR in HAs has been pioneered by Steelink[5] and Senezi[6] followed by many groups; for reviews of the extended literature see refs 6 and 19 and references therein. EPR spectroscopy provides direct evidence that the indigenous radicals are intimately related to the humification process in nature.[1,2,19] All the EPR data published within the past 40 years are based on conventional X-band EPR spectrometers[2,5,11,12,19] operating at ∼9 GHz, where the radicals are detected for magnetic fields around 3400 G. Usually three parameters are made available by the X-band EPR spectra, i.e., the g value, line width, and spin concentration per gram of HA. The fundamental EPR characteristics of the indigenous radicals are (a) their isotropic g values are usually in the range of 2.003−2.005[2,7,19] with a line width of 4−6 G and (b) the concentration of the radicals is pH dependent, showing a steep increase at pH > 7.[11,16,19] Hyperfine splitting is usually not resolved for humic acids except in rare cases.[19]

The g values of organic radicals are directly related to the electronic structure of the molecule and can serve as a sensitive probe of the structure of the radical and its immediate environment. However, the relative g variation of most organic radicals and their **g** anisotropy rarely exceed $10^{-4}-10^{-3}$ in terms of g value. In the case of more than one radical with similar g values and properties, it is rather difficult to resolve their overlapping EPR spectra with a conventional X-band EPR spectrometer.

The limitations encountered at the X-band can be largely overcome by performing EPR experiments at higher microwave frequencies/high magnetic fields, i.e., by high-field EPR (HFEPR); see Scheme 1. One of the principal advantages of HFEPR is the possibility to achieve complete resolution of the **g** tensor anisotropy for $S = 1/2$ systems[21] due to the increase of ΔB of two resonances at g_1 and g_2, see Scheme 1, with increasing magnetic field (eq 1). In practice this is achievable because often no noticeable line broadening occurs with increasing magnetic

* To whom correspondence should be addressed. E-mail: ideligia@cc.uoi.gr (Y.D.); sun@herode.saclay.cea.fr (S.U.).
† University of Ioannina.
‡ CEA Saclay.

10.1021/jp0717692 CCC: $37.00
Published on Web 10/19/2007

SCHEME 1: Schematic Representation of the Principle of High-Frequency/High-Field EPR Spectroscopy[a]

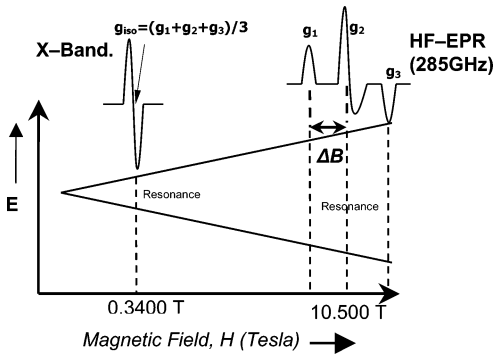

[a] The isotropic g value which is resolvable at X-band EPR is the average of the three components of the **g** tensor which can be fully resolved by high-field EPR.

$$\Delta B = \frac{h\nu}{\mu_B}\left(\frac{1}{g_1} - \frac{1}{g_2}\right) \quad (1)$$

field. In addition, HFEPR allows the resolution of signals that overlap at lower frequencies. Equation 1 shows that the spectral resolution increases linearly as a function of the microwave frequency ν.

In the present work we have transferred the HFEPR technique, currently used for radicals in biological systems, to HAs. In HFEPR we use high magnetic field/high frequency to measure the entire **g** tensor, rather than just the isotropic g value identified as the average of the three **g** tensor components, $g_{iso} = (g_1 + g_2 + g_3)/3$. It has been shown that accurately measured **g** tensors by HFEPR can be used to characterize radical centers and their interactions with their local environment (for examples see ref 21).

Here we present the first 285 GHz/10 T HFEPR spectra and accurate measurements of the **g** tensors of the radical centers of HAs. Various well-characterized HAs from diverse geographical locations were studied by HFEPR as a function of the pH. The aims of the present work are (a) to obtain insight into the electronic structure of the indigenous radicals of humic acids, (b) to study the influence of basic physicochemical parameters such as pH and geographical origin on the radical properties of humic acids, and (c) to demonstrate the applicability of HFEPR for the study of humic acids.

2. Materials and Methods

HFEPR Spectrometer. The HFEPR spectrometer used in the present work followed the design of Muller and coworkers.[22] The microwave source was a Gunn diode (Epsilon-Lambda, Geneva, IL) with a range of 90−100 GHz and a maximum output power of 90 mW. The frequency of the Gunn diode was tripled and doubled using an InP frequency tripler and doubler (Radiometric Physics, Menkenheim, Germany). The maximum resulting power was 3 mW. The microwave power absorbed by the sample was measured using a bolometer (QMC Instruments Ltd., United Kingdom). The magnetic field was generated using a superconducting 10.5 T magnet (Oxford Instruments, Oxon, England). The magnetic field at the sample was calibrated using an NMR gaussmeter and by EPR measurements using Mn(II) doped in magnesium oxide ($g = 2.00101$).[23] Field modulation was used to detect the signal. Sample temperature regulation was achieved using a helium flow cryostat. The accuracy of the temperature at the sample was estimated to be ±0.2 K.[24] All the other characteristics can be found elsewhere.[21]

In the present work, all measurements were carried out using the following conditions: 4.2 K, 285 GHz frequency, modulation amplitude 20 G, microwave power 300 μW. These conditions were selected because the signals were not saturated and they all behaved ideally.

X-band electron paramagnetic resonance spectra were recorded with a Bruker ESP300E spectrometer operating at X-band frequencies. Spectra were recorded at room temperature for powder samples or at cryogenic temperatures for liquid samples. The Bruker spectrometer with a 100 kHz magnetic field modulation was equipped with a Bruker NMR gaussmeter, ER 035M, and a Hewlett-Packard microwave frequency counter, HP 5350B. A Li/LiF standard was used for g value calibration.[11]

Sample Preparation. Four humic acids from diverse geographical locations were studied: HA1 isolated from a Polish coal,[11,16] HA2 obtained from a Greek soil using the standard International Humic Substances Society (IHSS) procedure,[11,25] HA3, a standard HA (leonardite) from the IHSS[25] (lot 1S104H-5), and finally HA4, a commercial peat HA from Fluka (lot 403608/1 53000) purified as described in ref 11.

Initially, for the preparation of each sample, the powder HA was dissolved at pH 12 (using NaOH) for 24 h under stirring. After dissolution, the stock solutions were brought to pH 6 (using HNO_3) and stored at 4 °C. The final HA concentration was 5 g/L. All samples were dissolved in ultrapure Milli-Q water produced by a Millipore Academic purifier. The commercial Fluka HA, i.e., HA-3, contained a large amount of Mn^{2+}, which at 285 GHz gives a strong signal at $g = 2$. To eliminate this contamination, a solution of 2 mL of HA (10 g/L) and ∼20 mM EDTA at pH 9 was stirred for 24 h and washed several times by using a dialysis tube to make sure that Mn^{2+} was washed away to a large extent. Through this treatment, even though the signal of Mn^{2+} was not fully removed, we were able to observe the formation of the radicals with increasing pH after subtraction of a reference Mn^{2+} signal. Careful comparison of the HFEPR spectra of the radicals showed that the dialysis procedure, apart from removing the undesired Mn^{2+}, did not alter the EPR radical signals of the sample.

Gallic acid (3,4,5-trihydroxybenzoic acid) was purchased from Aldrich.

EPR Sample Preparation. The EPR samples were prepared in aqueous solutions under ambient O_2 conditions, with no chemical oxidant added. Each sample was stirred under atmospheric O_2 at room temperature for 60 min.[11] Subsequently, each sample was frozen in liquid nitrogen and stored until the EPR spectrum collection. Several samples were prepared in this way, each one at a fixed pH value between 5 and 12. Typically eight samples at pH values between 5 and 12 were prepared using NaOH and HNO_3. Screening experiments showed that the particular acid or base used had no effect on the EPR signals. At each pH, the redox potential of the solution was monitored and found to vary linearly from −70 ± 5 mV at pH 5 to +150 ± 5 mV at pH 12, as expected.[20] It is emphasized that for the adjustment of pH no buffer was used since HA has its own buffering capacity.[1,11] To test the pH stability, the pH was measured after several freezing−thawing cycles. HA samples prepared at various concentrations, i.e., between 1 and 5 g/L HA, showed the same EPR spectra, except the signal intensity, which was increased as a function of HA concentration. Thus, for a better signal-to-noise ratio, we carried out the HFEPR experiments at 5 g/L HA. At a concentration of 5 g/L HA used in our experiments, the pH fluctuation did not exceed ±0.2 pH unit.

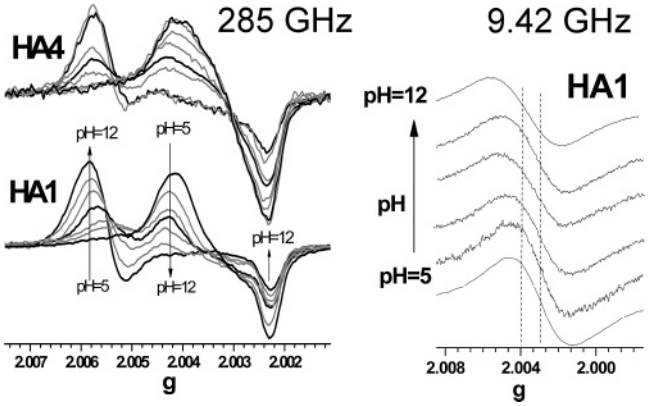

Figure 1. (Left panel) Experimental frozen solution HFEPR spectra of HA1 and HA4 at several pH values between 5 and 12 in steps of 1 pH unit. The vertical arrows serve as a visual aid for the pH-dependent spectral changes. (Right panel) EPR spectra (9.52 GHz) of HA1. The pH values from bottom to top are 5.0, 6.1, 7.8, 9.5, 10.8, and 12.0.

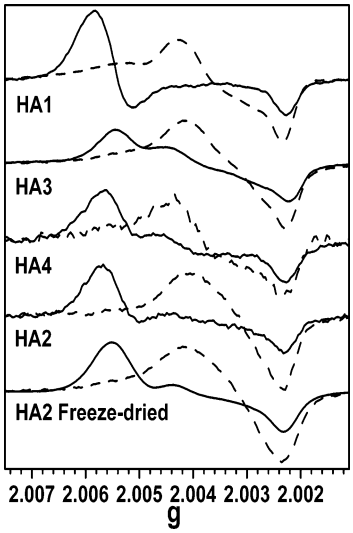

Figure 2. EPR spectra (285 GHz) for a frozen solution or freeze-dried powder of humic acid of various geographical origins: (solid lines) pH 12, (dashed lines) pH 5. The bottom spectra are for HA2 powder produced by freeze-drying HA2 at pH 5 or 12. Experimental conditions: $T = 4.2$ K, modulation amplitude 20 G.

3. Results

In Figure 1, left panel, we present HFEPR spectra for two humic acids, i.e., HA1 and HA4, as a function of the pH from 5 to 12 in steps of 1 pH unit. For comparison, the corresponding EPR spectra for HA1 recorded at the X-band, i.e., 9.42 GHz, are displayed in Figure 1, right panel. The same sample tube was used for the X-band EPR and the HFEPR spectra shown in Figure 1. The EPR signal intensity increased as a function of the pH, which is a well-known property of the radicals in humic acids.[2,6,11,16] For the sake of the comparison of the g values, normalized integrated EPR signal intensities are presented in Figure 1. The arrows in the HFEPR spectra in Figure 1 serve as a visual aid for the pH-dependent spectral changes. The progressive pH-dependent changes observed in Figure 1 were fully reversible (data not shown).

In Figure 1, we see that at acidic pH < 6 the HFEPR spectra extend from a g value of 2.0023 to $g = 2.0040$. At more alkaline pH the HFEPR spectra become different. At pH 6−8 the features change rapidly, see the arrows in Figure 1, left, while at pH $>$ 9 an anisotropic spectrum emerges. More particularly, at pH 12, a strong peak at $g = 2.0058$ is clearly resolved. On the other hand, the high-field edge of the spectrum at pH 12 remains near or below the free electron g value, $g = 2.0023$.

The corresponding X-band spectra manifest the pH effect as a small spectral shift, i.e., due to the average g value which is shifted toward higher values, i.e., from $g_{iso} \approx 2.0029$ at pH 5 toward $g_{iso} \approx 2.0040$ at pH 12, Figure 1, right panel. Analogous pH-dependent shifts at the X-band have been consistently reported in the literature for the vast majority of the HAs studied.[11,12,16,19] Thus, before we proceed to the analysis of the HFEPR data, we emphasize the significant enhancement of the spectral resolution and therefore the information content of HFEPR spectra relative to the X-band EPR spectra. The HFEPR spectral features show significant sensitivity to pH, while at the X-band this is manifested only as an upshift of the isotropic g value on going toward alkaline pH values.

Two Types of Spectra. A close examination of the pH dependence of the HFEPR spectra for HA1 in Figure 1 reveals the existence of two pseudo "isosbestic points". As we show in the following, this pattern was consistently observed for all the HA samples studied, although the exact magnetic field position of the isosbestic points differed somehow among different HA samples. As we show in the Theoretical Analysis section, these pseudo isosbestic points indicate that the HFEPR spectra consist of two subspectra which are interconverted as a function of the pH. For comparison, in Figure 2 we present 285 GHz HFEPR spectra of frozen aqueous solutions, at 4 K, of all the HAs at the two extreme pH values 5 and 12. The solid lines are HFEPR spectra recorded for the HAs at pH 12, while the dashed lines are HFEPR spectra recorded at pH 5. A striking observation in Figure 2 is that in all HFEPR spectra the same spectral pattern is observed at the same pH. The pH 5 HFEPR spectra show comparable, though not exactly identical, g values with limited **g** anisotropy. On going toward pH 12 all samples show HFEPR spectra which now become more anisotropic. At intermediate pH values all samples show two isosbestic points, like samples HA1 and HA4. At this point it is of relevance to emphasize that the samples studied here are of quite different geographical and geological origins. HA1 was isolated from a Polish coal, HA2 was from a Greek soil, HA3 was a leonardite IHSS HA, and finally, HA4 was a commercial peat HA.

Thus, overall, the HFEPR data show that despite the diverse origin and the acknowledged chemical complexity of HA, the HFEPR spectra exhibited a consistent pattern with two limiting types of EPR spectra. One type of EPR spectrum, herein termed "type I", prevails at pH < 6 and has limited **g** anisotropy. The second type, herein termed "type II", prevails at pH > 9 and has a more anisotropic **g** tensor. We adopt the term "type" to show that these two spectral forms do not have the same exact g values in all HA samples.

***g* Values.** The g values estimated for the spectra at pH 5 for type I and pH 12 for type II are listed in Table 1. Type I has principal g values $g^{I}_{x} = 2.0032 \pm 0.0002$, $g^{I}_{y} = 2.0032 \pm 0.0002$, and $g^{I}_{z} = 2.0023 \pm 0.0001$. Type II has g values $g^{II}_{x} = 2.0057 \pm 0.0002$, $g^{II}_{y} = 2.0055 \pm 0.0002$, and $g^{II}_{z} = 2.0023 \pm 0.0001$. Limited variations in the g values, i.e., on the order of 10^{-4}, are observed among the type I signals of the various HAs and similarly among the type II signals of the various HAs.

A second striking finding is that, despite the diverse origin of our HA samples, the HFEPR spectra show a surprisingly simple reversible acid−base behavior. As we show in the following, for each HA sample the spectral changes observed as a function of the pH are due to an interconversion between type I and type II spectra.

Freeze-Dried HA. The HFEPR spectral features observed for HA in aqueous solution are also observed for powdered HA,

TABLE 1: *g* Values and p*K* Values Obtained by the Theoretical Analysis of the HFEPR Spectra for Humic Acids

	g tensor[a] type I g_x, g_y, and g_z and type II g_x, g_y, and g_z	p*K* value[b]
HA1	$g^{I}_x = 2.0032$, $g^{I}_y = 2.0032$, $g^{I}_z = 2.0023$; $g^{II}_x = 2.0058$, $g^{II}_y = 2.0056$, $g^{II}_z = 2.0023$	8.8
HA2	$g^{I}_x = 2.0031$, $g^{I}_y = 2.0031$, $g^{I}_z = 2.0023$; $g^{II}_x = 2.0056$, $g^{II}_y = 2.0055$, $g^{II}_z = 2.0023$	9.2
HA3	$g^{I}_x = 2.0031$, $g^{I}_y = 2.0031$, $g^{I}_z = 2.0023$; $g^{II}_x = 2.0055$, $g^{II}_y = 2.0052$, $g^{II}_z = 2.0023$	9.0
HA4	$g^{I}_x = 2.0030$, $g^{I}_y = 2.0030$, $g^{I}_z = 2.0023$; $g^{II}_x = 2.0057$, $g^{II}_y = 2.0055$, $g^{II}_z = 2.0023$	8.9
HA2 freeze-dried	$g^{I}_x = 2.0030$, $g^{I}_y = 2.0030$, $g^{I}_z = 2.0023$; $g^{II}_x = 2.0055$, $g^{II}_y = 2.0053$, $g^{II}_z = 2.0023$	

[a] Error: $g_{x,y}$, ±0.0002; g_z, ±0.0001. [b] Error: ±0.2. The listed p*K* values are pH values where the weight factors f_1 and f_2 in eq 2 become equal, $f_1 = f_2 = 0.5$, derived from the fit to the spectra, according to the method exemplified in Figure 3. The p*K* for each HA sample can also be deduced directly from the crossing points in Figure 4.

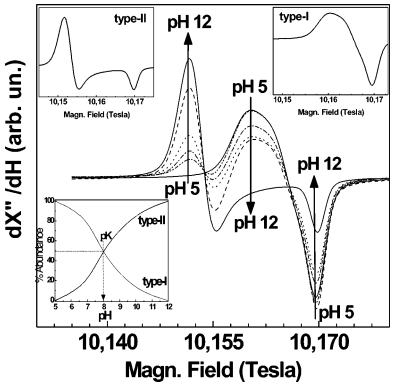

Figure 3. Theoretical HFEPR spectra calculated as a function of the pH by using eq 2. The spectra shown have been calculated using a p*K* value of 8.0, for pH 5.0, 7.0, 8.0, 9.0, 10.0, and 12.0. The vertical arrows are guides to the eye, showing the direction from pH 5 toward pH 12. Insets: (left) theoretical type I HFEPR spectrum dominant at low pH with principal *g* values $g^{I}_x = 2.0032$, $g^{I}_y = 2.0032$, and $g^{I}_z = 2.0023$; (right) theoretical type II HFEPR spectrum dominant at high pH with *g* values $g^{II}_x = 2.0057$, $g^{II}_y = 2.0055$, and $g^{II}_z = 2.0023$. The theoretical spectra, type I and type II, shown in the insets, were used as S_1 and S_2, respectively, in eq 2. Their relative abundance (%) at each pH is shown in the bottom inset. At pH = p*K* the contributions from type I and type II spectra are equal, $f_1 = f_2 = 50\%$.

Figure 2, bottom spectra, obtained by freeze-drying HA2 samples in solution poised at pH 5 or 12. In Figure 2 we observe that the type I spectrum is resolved in HA2 obtained by freeze-drying HA2 in solution at pH 5. Similarly the type II spectrum is resolved in freeze-dried HA at pH 12. The spectral features of the freeze-dried samples show small differences from the corresponding spectra of HA2 in solution. We consider that these might reflect either differences in the local concentration of H^+ or differences in the local concentration of other positive charges in the dried sample. It is well-known that H-bonds and/or local positive charges can cause shifts in the *g* values of organic radicals which are detectable by HFEPR,[21,25] e.g., such as those observed in Figure 2. Alternatively, conformational changes of the HA macromolecule during the freeze-drying procedure might be responsible for the small spectral shifts. The important observation however is the persistence of the two EPR signal types in the powder form as well as in solution.

Theoretical Analysis of the HFEPR Spectra. All the HFEPR spectra recorded for the various HAs can be simulated by a linear combination of the two limiting spectra, type I and type II. The simulation process is exemplified in Figure 3. Initially two theoretical spectra, indicated as type I and type II, see the upper insets in Figure 3, were generated by simulating the experimental HFEPR spectra at pH 5 and 12, respectively, i.e., with the *g* values of the type I and type II spectra listed in Table 1.

On the basis of the experimental observation of the reversible pH-dependent transition from type I to type II spectra, we assume that each spectrum at any pH is a linear combination of these two limiting spectral forms. Mathematically this is described by the formula

$$I = (f_1 S_1) + (f_2 S_2) \tag{2}$$

with

$$f_1(\mathrm{pH}) = \left[\frac{10^{\mathrm{p}K-\mathrm{pH}}}{1 + 10^{\mathrm{p}K-\mathrm{pH}}}\right]$$

$$f_2(\mathrm{pH}) = 1 - f_1(\mathrm{pH})$$

where S_1 and S_2 symbolize the type I and type II spectra, respectively, and f_1 and f_2 stand for the relative percentage of the type I and type II spectra, respectively. The fractions f_1 and f_2 vary between 0 and 1, with $f_1 + f_2 = 1$.

The derivation of this formula is based on the following model: (a) Each spectrum at any pH consists of a linear superposition of two weighted fractions of two spectra corresponding to type I and type II. (b) The two spectral forms, type I and type II, are the only components contributing. Mathematically this is expressed as $f_1 + f_2 = 1$ in formula 2. (c) The weight factor f_1 is a sigmoidal function of pH, parametrized by a single "p*K* value"; see expression 2, which is adjustable, i.e., determined by the fit to the experimental data.

The justification of the validity of the model is based (a) on the observation of only two types of spectra, type I and type II, in the experimental spectra and (b) their reversible interconversion as a function of the pH, evidenced by the isosbestic points. The use of the term "p*K*" is adopted here in the mathematical formulation of f_1 and f_2 since it describes a pH-dependent transition between two limiting states. Its physical meaning, i.e., with regard to deprotonation events, will be further analyzed in the Discussion.

Despite its simplicity, as we show here this approach appears to provide a successful working mathematical model; e.g., compare Figure 3 with Figure 1, left panel. By comparing Figures 3 and 1, we see that the pH effect on the experimental HFEPR spectra, Figure 1, can be simulated by the theoretical spectra in Figure 3. According to the theoretical spectra in Figure 3, at pH 5 the type I spectrum prevails while at pH 12 the characteristics of the type II spectrum dominate. In Figure 3 each spectrum shown, at any intermediate pH, has been generated as a weighted sum of the spectra type I and type II using formula 2 for a p*K* value of 8.0. The relative percentage of the f_1 and f_2 fractions is plotted as a function of the pH in the lower inset in Figure 3. As can be seen, the value of the parameter p*K* describes the pH value where the weight factor of each subspectrum, f_1 and f_2, is $f_1 = f_2 = 50\%$.

Equally important, in this model, the two characteristic isosbestic points are well explained as being due to the crossing of the derivative line of one spectrum with the flat part of the

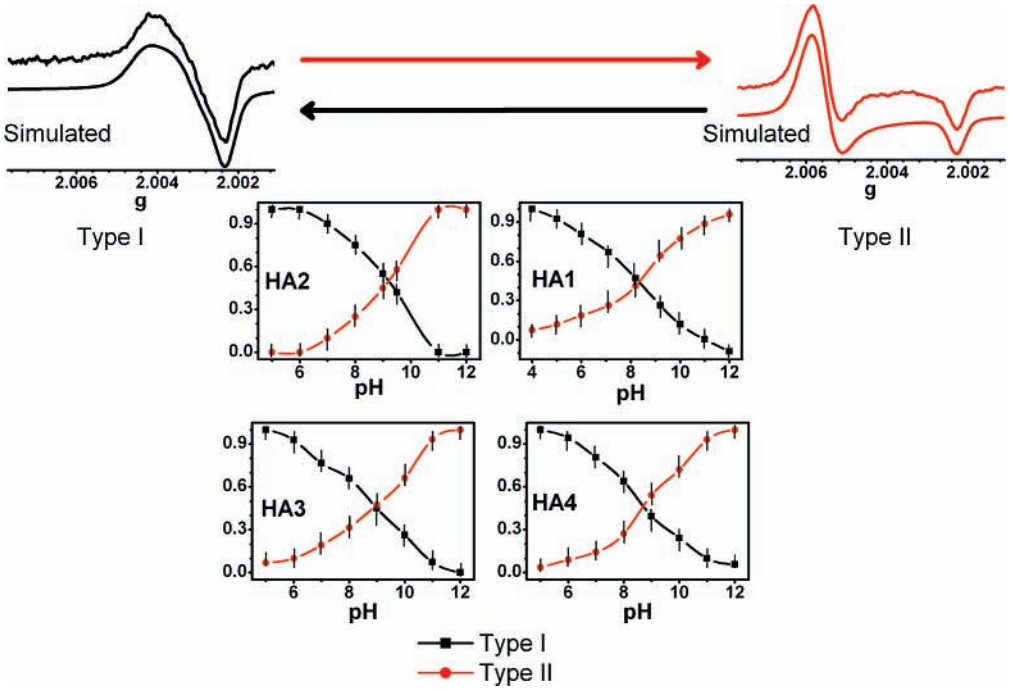

Figure 4. Deconvolution of the experimental HFEPR spectra as a weighted sum of the spectral type I and type II according to the method described in Figure 3. The crossing point in each figure occurs at the p*K* value used in formula 2, listed in Table 1.

other spectrum; compare Figures 3 and 1. The $g = 2.0023$ troughs, i.e., at a magnetic field near 10.7 T, of both the type I and type II spectra overlap, therefore the persistence of this feature in all spectra.

In this way, by adjusting only the p*K* parameter, the theoretical spectra can describe successfully the experimental HFEPR spectra. The complete speciation analysis derived for the four HAs, according to the theoretical model, is displayed in Figure 4. The pH profiles of the fractions f_1 and f_2 obtained from the deconvolution of the spectra, see Figure 4, all exhibited a single crossing point when type I vs type II spectra were in a 1:1 ratio. The crossing points of all the HAs occurred within a narrow pH range between 8.3 and 9.0; see Figure 4. These crossing points provide the p*K* values and can be read from the speciation plots in the panels in Figure 4. Therefore, the spectral changes observed in the HFEPR spectra as a function of the pH can be assigned to the interconversion of the type I spectrum to the type II spectrum with a p*K* value in a narrow pH range, 8−9. The obtained *g* and p*K* values are summarized in Table 1. Their physical meaning will be discussed in the following.

4. Discussion

The present data reveal that HFEPR can provide a wealth of novel information with regard to the radical properties of HAs. The **g** tensors are fully resolved, and this allowed a detailed deconvolution of the EPR spectra in their components. Despite the acknowledged notorious complexity of humic acids, all the studied HA samples from largely diverse origins contain the same two main types of indigenous radicals, type I and type II. More interestingly, the two types of radicals show a simple acid−base interdependence. The pH dependence of the radical EPR signals in HAs was largely known from X-band EPR,[5,6,19] from the shift in the g_{iso} values. However, the origin and significance of this phenomenon could not be further analyzed on the basis of the X-band data. The present HFEPR data show that this *g* shift originates from a specific pH-controlled interconversion of the type I and type II forms, rather than a random variation of the *g* values, i.e., for example, due to sample heterogeneity.

The fact that the spectral changes were fully reversible as a function of pH and redox potential demonstrates that the two types of spectra reflected two stable fundamental forms that were in equilibrium with each other and differentiated only by protonation−deprotonation phenomena with a characteristic p*K* near 8−9. The striking finding was that in all HAs from diverse geographical origins on Earth the main features and trends observed for the two limiting pH values are consistently shown.

Equally importantly, the two limiting types of spectra were also observed in solid samples. The observed stability of both these types of radicals, e.g., for over 3 months, concurs with the current concept of the stability of the indigenous radicals in humics.

Structural Assignment: Model Compounds. Given the largely unknown structure and detailed composition of HAs, any attempt for a structural assignment of the two types of radicals should be treated with great caution. Structural assignments of the radicals based on X-band EPR have been discussed in authoritative reviews; see, for example, refs 2 and 19. On the other hand, however, since this is the first literature report for high-resolution EPR spectra for HAs on the interconversion of the two types of stable radicals, it is tempting to discuss some reasonable possibilities toward their structural assignment. In this context in Figure 5, we present a limited collection of HFEPR spectra of organic radicals as an aid for the discussion of the spectral features. These include a semiquinone radical, a β-carotene radical, and a pheophytin anion radical which are well-known to abound in natural systems such as plants (Figure 5).[21]

The g_z values, the lowest **g** tensor component, for both type I and type II radicals in HAs were at or below the free electron *g* value of 2.0023; see Table 1. Since this typically occurs when the unpaired electron is in a p-orbital or a system of conjugated p-orbitals,[21,26] it can be concluded that both types of HA radical centers were likely to be π-type. This conclusion is in agreement

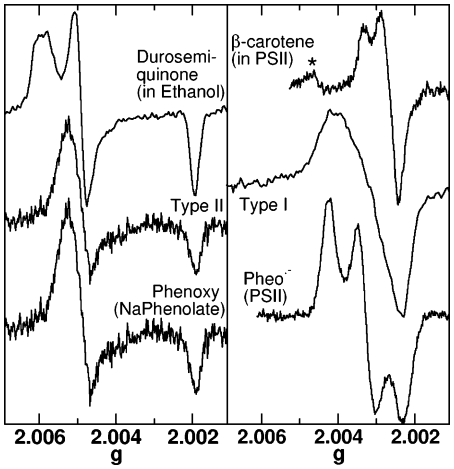

Figure 5. Comparison of the HFEPR spectra of HA type II (left) with oxygen-containing aromatic radicals and type I (right) with radicals with extended delocalization. Data were taken from ref 21.

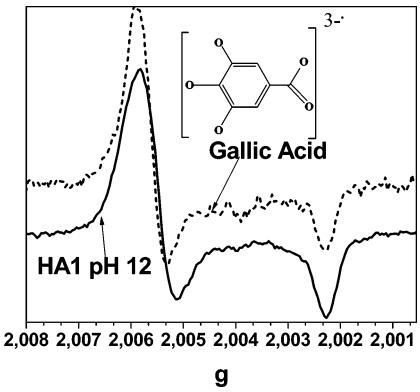

Figure 6. Comparison of the HFEPR spectra of HA type II (solid line) with the radical generated on gallic acid in aqueous solution under O_2, at pH 12.0 (dotted line). Inset: structure of gallic acid. Experimental conditions are as in Figure 1.

with the original EPR works; see refs 2 and 19 and references therein.

The relatively small **g** anisotropy defined as

$$\mathbf{g}\ \text{anisotropy} = \left|\frac{g_x - g_y}{g_z}\right|$$

of the low pH form indicated that the unpaired electron spin density either was constrained to a carbon atom or was highly delocalized. By contrast, the larger **g** anisotropy of the high-pH form suggested significant spin density was on one or more oxygen or nitrogen atoms.[21,26] Similar **g** anisotropies were observed in HFEPR spectra for semiquinones in alcohols and radical centers in optically illuminated crystalline sodium phenolate hydrate (Figure 5, right).

Thus, it appears that phenolic molecules have EPR spectra similar to those of the type II radicals in humic acids. Recently, we have shown that the radical properties of gallic acid (*g* value, pH dependence, reaction with metals such as Pb) bear relevance to the radicals of HA.[11] Of pertinence to the present HFEPR data is the observation that gallic acid forms radicals at alkaline pH > 8 in the presence of ambient O_2 with *g* values comparable to those of humic acids.[11] In this context we have recorded HFEPR spectra for gallic acid at pH 12.0 formed under ambient O_2. In Figure 6 we observe that the HFEPR spectra of gallic acid bear striking similarity to the HFEPR spectrum type II of HA1. Thus, the present HFEPR data enforce our previous observation[11] that gallic acid can serve as a good model of the radical of HA. The present data provide a specific guidance showing that gallic acid is well suited for modeling type II centers. Further detailed HFEPR investigation of the radical properties of gallic acid are in progress.

Thus, the present data, *g* values and comparison with model compounds, provide strong evidence that the type II radicals in HAs are localized on phenolic molecules. This is consistent with the finding of the p*K* value near pH 8−9 for the formation of the type II radical in all HAs studied. In aqueous solution at alkaline pH deprotonation of the phenolic OH group is a key step for radical formation.[1,11,19,21] Literature data from H-binding studies provide ample evidence that phenolics are among the main building blocks of HAs with p*K* values in the range 8−9.[1,3] On the basis of these observations, as a minimal approach for the structural assignment, we consider that the type II radicals are due to phenolic groups in HAs. The molecular nature of type I radicals is more difficult to probe. One simple model for the observed pH dependence of the type I and type II radicals is that both forms share a common site that has an acidic oxygen. When protonated, the spin density would be localized on the nearby carbons, but upon deprotonation, it would shift and localize onto the heteroatom. Other models that involve two different sites, i.e., one for each type of radical, where spin density is shifted by pH-dependent conformational changes, cannot be ruled out at present. This structural model, although speculative at the moment, provides testable working hypotheses which deserve further investigation, e.g., by HFEPR studies of fractionated HAs and/or model polymers.

5. Conclusion

Two types of spectra, type I and type II, are consistently resolved for all the HAs studied, which prevail reversibly at acidic and alkaline pH in aqueous solution as well as in solids. Given that the radicals are formed under ambient O_2, this demonstrates that these two types of radicals are most likely to be formed in the real environment in soil of varying hydration as well as in dissolved organic matter.

Although the pH-dependent shift of the isotropic *g* values for the radicals in HAs was known from previous X-band EPR studies, HFEPR provides a detailed picture of the origin of this *g* shift, revealing that it originates from a pH-dependent interconversion of two types of indigenous radicals. In this respect our results reported here show that high-field EPR can shine new light on the chemistry of these elusive species.

Acknowledgment. We thank the PICS program of the CNRS (Grant No. 1973/Greece) and the ESF Cost P15 action for financial support.

References and Notes

(1) Stevenson, F. J. *Humus Chemistry: Genesis, Composition and Reactions*, 2nd ed.; John Wiley and Sons: New York, 1994.

(2) Senesi, N.; Loffredo, E. The Chemistry of Soil Organic Matter. In *Soil Physical Chemistry*; Sparks, D. L., Ed.; CRC Press: Boca Raton, FL, New York, 1999; pp 239−370.

(3) Tipping, E. *Cation Binding by Humic Substances*, 1st ed.; Cambridge University Press: Cambridge, U.K., 2002.

(4) Rex, R. W. *Nature* **1960**, *188*, 1185−1186.

(5) Steelink, C.; Tollin, G. *Biochim. Biophys. Acta* **1962**, *59*, 25−34.

(6) Senesi, N.; Steelink, C. In *Humic Substances II: In Search of Structure*; Hayes, M. H. B., MacCarthy, P., Malcolm, R. L., Swift, R. S., Eds.; Wiley: New York, 1989; pp 373−408.

(7) Lovley, D. R.; Coates, J. D.; Blunt-Harris, E. L.; Phillips, E. J. P.; Woodward, J. C. *Nature* **1996**, *382*, 445−448.

(8) Alberts, J. J.; Schindler, J. E.; Miller, R. W. *Science* **1974**, *184*, 895−896.

(9) Sunda, W. G.; Kieber, D. J. *Nature* **1994**, *367*, 62−65.
(10) Zepp, R. G.; Baugham, G. L.; Schlotzhauer, P. F. *Chemosphere* **1981**, *10*, 109−117.
(11) Giannakopoulos, E.; Christoforidis, K. C.; Tsipis, A.; Jerzykiewicz, M.; Deligiannakis, Y. *J. Phys. Chem. A* **2005**, *109*, 2223−2232.
(12) Paul, A.; Stösser, R.; Zehl, A.; Zwirnmann, E.; Vogt, R. D.; Steinberg, C. E. W. *Environ. Sci. Technol.* **2006**, *40*, 5897−5903.
(13) Scott, D.T.; McKnight, D. M.; Blunt-Harris, E. L.; Kolesar, S. E.; Lovley, D. R. *Environ. Sci. Technol*. **1998**, *32*, 2984−2989.
(14) Kamiya, M.; Kameyama, K. *Chemosphere* **1998**, *36*, 2337−2344.
(15) Schnitzer, M.; Levesque, M. *Soil Sci*. **1977**, *127*, 140−145.
(16) Jerzykiewitcz, M.; Drozd, J.; Jezierski, A. *Chemosphere* **1999**, *39*, 253−268.
(17) Wilson, S. A.; Weber, J. H. *Chem. Geol.* **1979**, *26*, 345−354.
(18) Wilson, S. A.; Weber, J. H. *Anal. Lett.* **1977**, *10*, 75−84.
(19) Senesi, N. In *Applications of ESR Spectroscopy in Soil Chemistry*; Stewart, B. A., Ed.; Advances in Soil Science 14; Springer-Verlag: New York, 1990; pp 77−130.
(20) Struyk, Z.; Sposito, G. *Geoderma* **2001**, *102*, 329−346.
(21) Un, S.; Dorlet, P.; Rutherford, A. W. *Appl. Magn. Reson.* **2001**, *21*, 341−361.
(22) IHSS Web site reference. Isolation protocol. The samples were characterized by UV−vis (E_4/E_6 ratio), elemental analysis, FT-IR spectroscopy, and fluorescence spectroscopy; see refs 11 and 16 for details.
(23) Muller F.; Hopkins, M. A.; Coron, N.; Grynberg, M.; Brunel, L.; Martinez, G. *Rev. Sci. Instrum.* **1989**, *60*, 3681−3684.
(24) Burghaus, O.; Rohrer, M.; Götzinger, T.; Plato, M.; Möbius, K. *Meas. Sci. Technol.* **1992**, *3*, 765−774.
(25) Ivancich, A.; Mattioli, A. T.; Un, S. *J. Am. Chem. Soc.* **1999**, *121*, 5743−5763.
(26) Stone, A. J. *Proc. R. Soc. London, A* **1960**, *271*, 424−434. (b) Stone, A. J. *Mol. Phys.* **1963**, *7*, 311−316. Stone, A. J. *Proc. R. Soc. London, A* **1963**, *271*, 424−434. (b) Stone, A. J. *Mol. Phys.* **1963**, *6*, 509−515. (c) Stone, A. J. *Mol. Phys.* **1963**, *7*, 311−316. (d) Angstl, R. *Chem. Phys.* **1989**, *132*, 435−442.